Journal of Microscopy, Vol. 189, Pt 1, January 1998, pp. 79–89.
Received 21 April 1997; accepted 11 August 1997

A comparative study of thin coatings of Au/Pd, Pt and Cr produced by magnetron sputtering for FE-SEM

I. STOKROOS, D. KALICHARAN, J. J. L. VAN DER WANT & W. L. JONGEBLOED
Laboratory of Cell Biology and Electron Microscopy, University of Groningen, Oostersingel 69/2, 9713 EZ Groningen, The Netherlands

Key words. Au/Pd, Cr, field emission scanning electron microscopy, high-vacuum evaporation, planar magnetron sputtercoating, Pt.

Summary

Visualization of structural details of specimens in field emission scanning electron microscopy (FE-SEM) requires optimal conductivity. This paper reports on the differences in conductive layers of Au/Pd, Pt and Cr, with a thickness of 1·5–3·0 nm, deposited by planar magnetron sputtering devices. The coating units were used under standard conditions for source–substrate distance, current, HT and argon pressure. Carbon films, deposited by high-vacuum evaporation on small, freshly cleaved pieces of mica, were used as substrate and mounted on copper grids for TEM and SEM inspection. Au/Pd, Pt and, to a lesser extent, Cr coatings varied in particle density, size and shape. Au/Pd coatings have a slightly more granular appearance than Cr and Pt coatings, but this is strongly dependent on the type of sputtering device employed. In FE-SEM images there is almost no difference in contrast and particle size between the Au/Pd layer and the Pt layers of a similar thickness. The nuclei of Au/Pd are rather small with almost no growth to the sides or in height, making Au/Pd coatings a good alternative to chromium and platinum for FE-SEM of biological tissues because of its higher yield of secondary electrons.

Introduction

The use of a scanning electron microscope with field-emission cathode (FE-SEM) has considerable consequences for the specimen preparation. Artefacts resulting from poor preservation and conductivity of biological tissues are rapidly observable in FE-SEM. In the past the resolution of the SEM was in the order of 3–7 nm; now, resolutions of 1·5 nm or better can be achieved with FE-SEM. Therefore the quality and thickness of the coating material, coating techniques and their reproducibility have to be adapted to a higher level of performance.

Correspondence to: Dr W. L. Jongebloed, fax: 31-(0)50 3632515, E-mail: w.l.jongebloed@med.rug.nl

In past decades of TEM research and in freeze break/freeze etch experiments platinum has often been used as shadow material at replication, owing to the absence of any structure of the platinum nuclei (Gross *et al.*, 1984, 1985, 1990; Müller *et al.*, 1985).

With the introduction of a cryo-transfer system onto our FE-SEM, we were confronted with the relatively fine grains of the Au/Pd layer applied to the fractured yeast surface at −120 °C using the Denton planar magnetron sputtering. Because there is a tendency these days to coat specimens with chromium, giving extremely small grains and an even distribution of chromium nuclei in the coating layer, there is reason enough to compare different coating materials, procedures and instruments. So we were interested in the properties of Au/Pd coatings in comparison with Cr and Pt coatings for use in the FE-SEM for hard and soft biological tissue (Oxford Instruments, 1995).

The conductive coatings compared in this study, have an average thickness of 1·5–3·0 nm; this means that they do not belong to the category of ultrathin coatings which are considered to have thicknesses of 1·0 nm or less. The production of those extremely thin deposits requires a much more tightly controlled gas pressure and purity, molecular weight of the ionized gas and accelerating voltage; moreover, the temperature of the substrate is also rather important. It is known that the structure of a coating layer is dependent on several parameters such as coating material, coating layer thickness, sputtering system, vacuum conditions and temperature (ambient or cryo). Besides these conditions, the type of substrate (composition and topography) also plays an important role in the quality and homogeneity of the coating. These parameters affect the way the metal nuclei stick to the substrate and hence determine the chances of nuclei migration and agglomeration (Peters, 1986; Ruben, 1989; GATAN, 1997).

The presence of a thin conductive coating is necessary when the conductivity of the sample is insufficient; this certainly will be the case at higher accelerating voltages

used with biological samples. Moreover, the presence of a conductive layer stimulates the generation of secondary electrons, particularly at the surface of the sample, the type 1 secondary electrons. A conductive coating is then appropriate only when the topographic features of the sample are not significantly enlarged or obscured by the metal coating. A conductive coating should therefore be as thin as possible without masking surface details. It should be continuous, conductive and have a high secondary electron emission coefficient leading to a good contrast in the image. The optimal situation will be attained when the metal film is of minimal thickness, contains grains which have almost no surface mobility, so that no decoration effects will impair the visibility of surface phenomena, and are smaller than the probe diameter (Peters, 1984, 1986).

Biological tissues often have a rather uneven surface topography, therefore ultrathin coatings are less suitable because they do not fulfill the need for a continuous layer across large areas of the sample. In many cases a treatment with so-called noncoating techniques, to be used at high (5–25) and low (1–5) kV, increasing the amount of bound osmium or other heavy metals to the structures, is more appropriate, overcoming the need for an external conductive coating (Kalicharan *et al.*, 1992; Jongebloed *et al.*, 1994).

The purpose of this study is to compare the fine structure of different coatings deposited onto carbon film by planar magnetron sputtering using instruments from different manufacturers.

Materials and methods

In this study the following materials were used: Au/Pd, Pt, Pt/C and Cr; the coatings were deposited on a carbon film substrate mounted on 3-mm TEM copper grids. The carbon film was evaporated on freshly cleaved mica. The coatings onto copper grids were observed in SEM and TEM for evaluation of the particle size, shape, distribution and stability in layers with a thickness of 1·5–3·0 nm. Observations were carried out directly after deposition of the layers and also after 1 week; within this period no changes were noticed.

Microscopes

a JEOL FE-SEM 6301F (with cold field emission cathode), employed at 5 and 15 kV, respectively, working distance ≈ 6 mm, beam current 10^{-11} A; images were produced on roll film 6×7 cm.
b Akashi TEM 002A with tungsten cathode, employed at 100/120 kV, with the objective lens unit set in the high-resolution mode; images were produced on $21/4 \times 31/4$ inch plates.

Evaporation-cq sputtering devices

1 *High vacuum evaporation unit,* type Balzers BAE 120, with turbomolecular pump and equipped with a quartz crystal thin film monitor, producing carbon films on mica by carbon rod resistance heating and an HT source to deposit a Pt/C coating.
2 *Ion beam sputter coating unit,* Ion Tech saddle field ion source EM microsputter Model B370 with ion beam source on an Edwards high-vacuum oil diffusion pump unit with Au/Pd target. Current: 5·0 mA at 8 kV, 2×10^{-5} mbar argon pressure and a fixed source–(rotating) substrate distance of 20 mm with Au/Pd target.
3 *Planar magnetron sputter coating devices*
a Denton, fitted with a cool anode grid as a subunit of the Oxford CT 1500 HF Cryo transfer system (Oxford Instruments, Cambridge, U.K.). Current 10 mA, 250 V DC, 5×10^{-4} mbar (high-purity) argon, Au/Pd and Pt targets used at 20 °C. and -120 °C; and a fixed source–substrate distance of 40 mm.
b Cressington 'cool' Turbo Sputter Coater 208 HR (Elektronen Optik Service GmbH, Dortmund, Germany). At short and long source–substrate distance, current 20 mA, 0·15 mbar (high-purity) argon, quartz crystal thin layer monitor.
c Fisons as subunit of the LT7400 Cryo preparation system (VG Microtech, Uckfield, East Sussex, U.K.) with HT power supply (300 V/50 mA DC current limiting supply), a separate SC500 'cool' sputter coater unit and in succession to the SC 500 the VG Microtech SC 7640 Polaron sputter coater with a circle-shaped target (1200, 800 and 600 V/DC variation was used). Pt targets employed in the SC500 and SC 7640 model at room temperature and in the cryo unit at the stage temperature of -120 °C.
d Xenosput XE200 (Edwards High Vacuum International, Cambridge, U.K.) used at standard source–substrate distance. A 70-mA current for 15 s was used for Cr and a 30-mA current for 10 s for Au/Pd to obtain a layer thickness of approximately 1·5 nm.

Most of the sputtering devices used did not have a film thickness measuring device; only the Balzers BAE 120 evaporation unit, the VG Microtech SC 7640 and the Cressington Coater 208 HR were equipped with a thin film monitor (QTFM). Thickness measurements of each layer were carried out with help of tables provided with the various instruments; the thickness was measured as a function of target–specimen distance, current and time. This is different from measurements with a single crystal QTFM because its measurement is dependent on the location with respect to the carbon substrate. Moreover it measures mass thickness, which is different from average metric thickness in the case where the coating is not continuous (Echlin, 1992). In order to check whether the method was reliable, we compared the results of our measurements with the data obtained from the instruments

using a film thickness measuring device. The conclusion was that for the relative measurement we carried out the method gave results that varied by 20–22%. This is in agreement with our starting position: to compare coatings of different materials produced with different sputtering devices at standard conditions set by the manufacturers. If differences in coating particle size and density were found for the same metal, this could be attributed to the particular construction of each instrument. To avoid differences due to variations in substrates all coatings were deposited on carbon film.

Results

1. Ion beam sputtered Au/Pd coatings on carbon film

As a comparison to the tests carried out with the various planar magnetron sputtering devices, a 3·0-nm Au/Pd layer

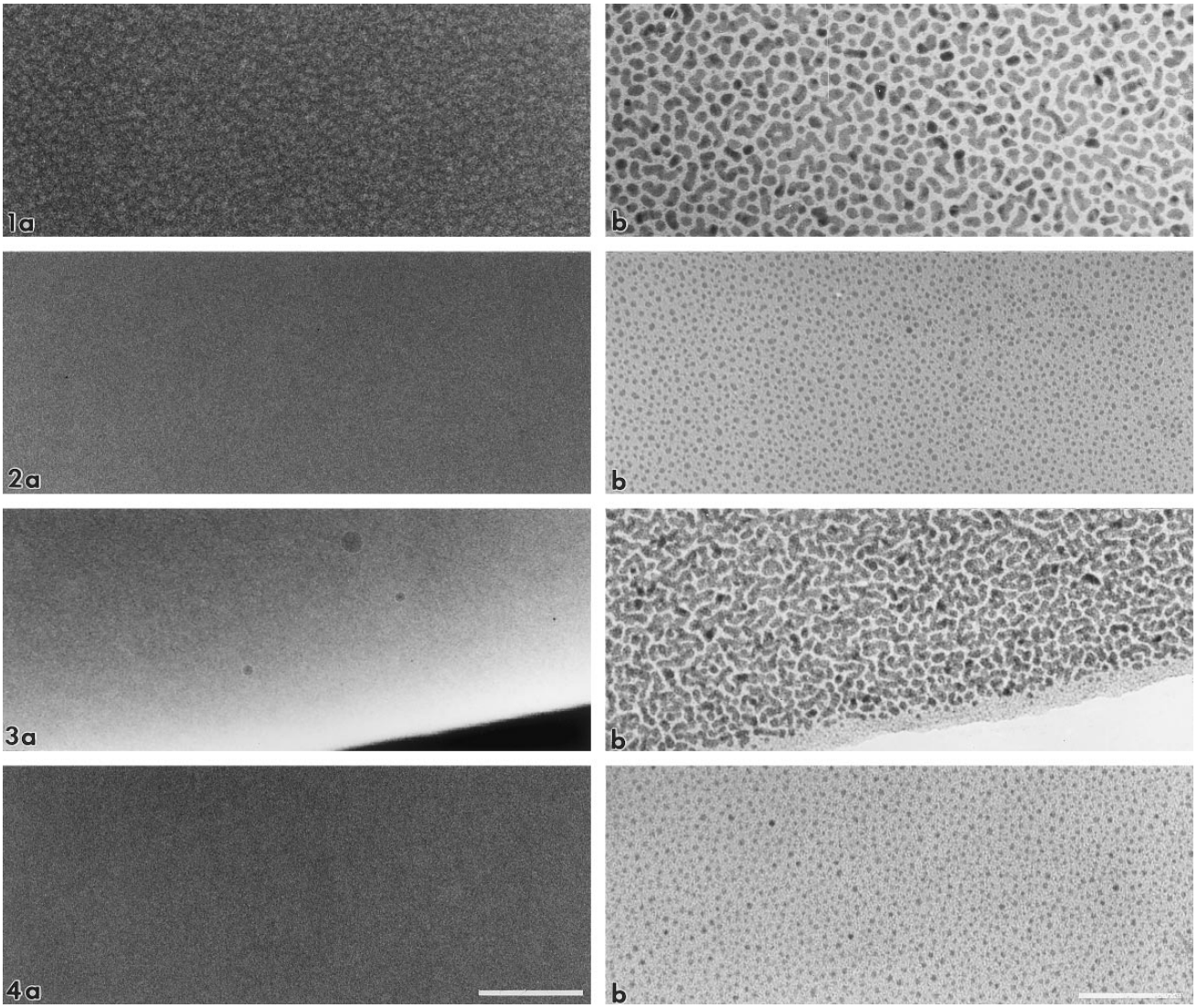

Fig. 1. Ion-beam sputtered (Ion Tech B-370) 3·0-nm Au/Pd layer on carbon, produced at RT; SEM (a) and TEM (b). Note rather small Au/Pd nuclei in an almost continuous layer. Scale bar (see Fig. 4) = 50 nm.
Fig. 2. Planar magnetron sputtered (Cressington 208 HR) 1·5-nm Au/Pd layer on carbon, produced at RT; FE-SEM, 15 kV (a) and TEM, 100 kV (b). Note slightly lower contrast in SEM with respect to Au; the mostly round nuclei have agglomerated in units closely packed together. Scale bar (see Fig. 4) = 50 nm.
Fig. 3. Planar magnetron sputtered (Denton-Oxford CT 1500HF Cryo Transfer System) 1·5-nm Au/Pd layer on carbon produced at − 120 °C; FE-SEM, 15 kV (a) and TEM, 100 kV (b). Note very small Au/Pd nuclei forming a continuous layer. Scale bar (see Fig. 4) = 50 nm.
Fig. 4. Planar magnetron sputtered (XE200 Xenosput) 1·5-nm Au/Pd layer on carbon produced at RT; FE-SEM, 15 kV (a) and TEM (b). Note the rather irregular shaped nuclei reasonable closely packed together. Scale bar = 50 nm.

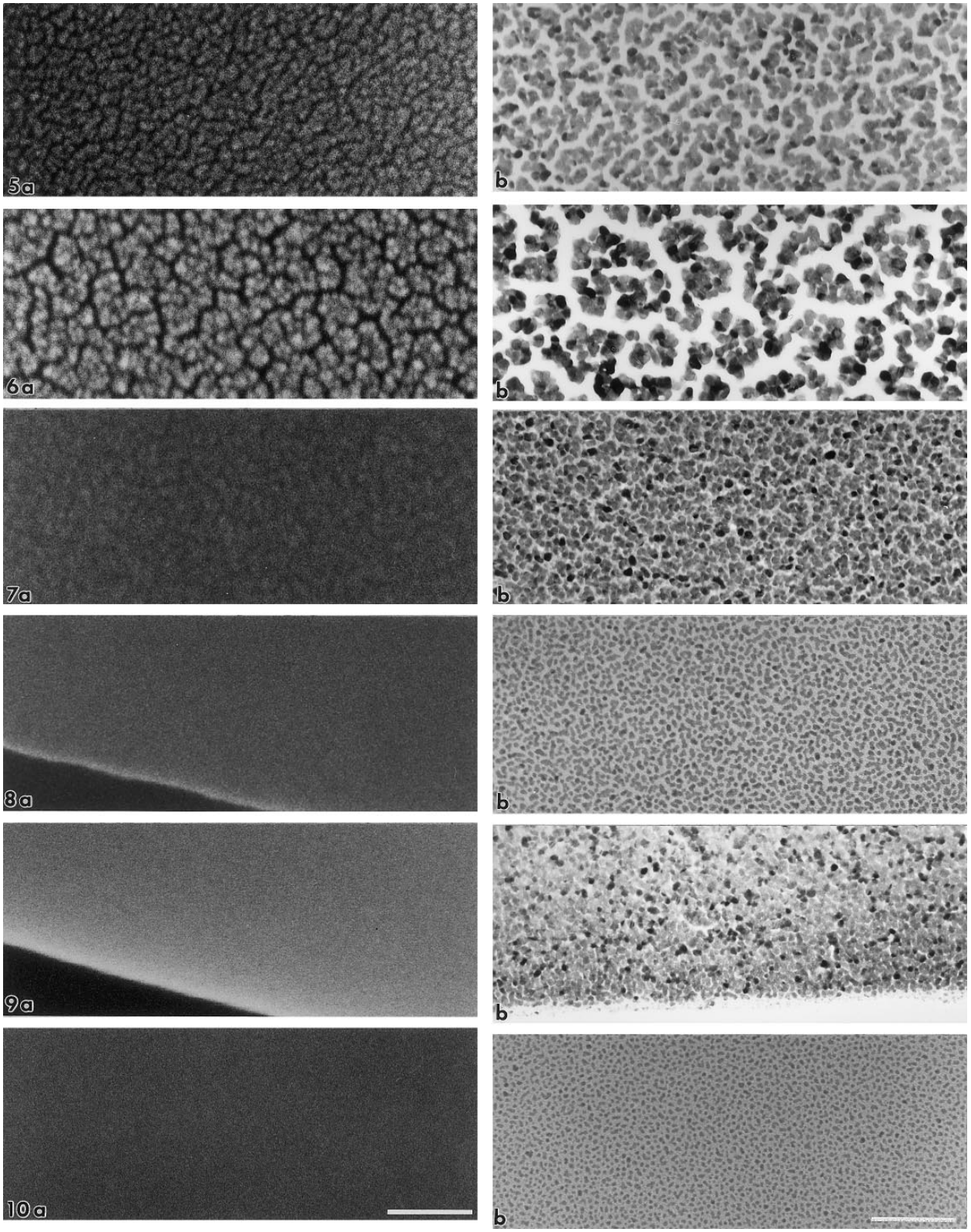
5a
b
6a
b
7a
b
8a
b
9a
b
10a
b

was produced with an ion-beam sputtering device (Ion Tech EM Micro-sputter coater B 370) on carbon film as substrate (Fig. 1). The grain size of the metal particles in the Au/Pd film is smaller than that of Au layers of comparable thickness. However, in FE-SEM the substructure of Au/Pd particles can be shown in this layer. In TEM the particles are rather densely packed but show a less uniform shape, between the relatively large particles very small particles are also found.

To investigate whether another sputtering method could produce coatings with smaller nuclei than obtained with an ion-beam sputtering device, layers of Au/Pd, Pt and Cr were deposited with various planar magnetron sputtering devices.

2. Magnetron sputtered Au/Pd coatings on carbon film

a With the Cressington 208 HR planar magnetron sputtering device a 1·5-nm Au/Pd was produced at room temperature and short deposition distance, as shown in the FE-SEM image of Fig. 2(a) and the TEM image of Fig. 2(b). The Au/Pd nuclei in this layer appear reasonably homogeneously divided and are smaller than those obtained in the ion-beam sputtered layer as shown in Fig. 1. No substructure due to Au/Pd nuclei is observable in the FE-SEM image; in the TEM image, however, a subdivision in particles is observable. The particles are rather small, though not very uniform in shape and size; the somewhat gray background of the TEM image suggests the presence of still smaller particles.

b With the Denton planar magnetron cold sputter device, as subunit of the Oxford Instruments CT1500 HF Cryo-Transfer system, at RT, a 1·5-nm Au/Pd layer was produced; almost no substructure due to Au/Pd nuclei is observable in the FE-SEM image (Fig. 3a). In the TEM image, however, the Au/Pd particles with a 'heterogeneous curved' appearance are closely packed with a minimum of space between the particles, as observable in Fig. 3(b). The background or open space between the particles is more clearer than that seen in Fig. 2.

c With the Xenosput XE200 a 1·5-nm Au/Pd layer was produced at room temperature. At first view the layer appears structureless, as observable in the FE-SEM image (Fig. 4a). In the TEM image, Fig. 4(b), the particles with a 'star-like' appearance are rather small and uniform in size. The open spaces are rather large, but given a closer look it seems that the background consists of very small particles closely packed together. The layer also shows a certain arrangement of particles as larger open units with a hexagonal shape. This is different, but comparable with the structure seen in Fig. 2(b).

3. Magnetron sputtered Pt coatings on carbon film

a With the Fisons planar magnetron sputter coater, as subunit of the LT 7400 Cryo preparation system for SEM, a 2·0-nm Pt layer was applied at low temperature (−120 °C). The FE-SEM image of Fig. 5(a) shows some substructure, the agglomerates are even larger than those of the ion-sputtered Au/Pd layer of Fig. 1. Observing the TEM image, Fig. 5(b), more carefully there is an indication that the individual particles have an angular shape, but otherwise are reasonably uniform in size and shape. There are rather large open spaces between the conglomerates.

b With the Fisons planar magnetron sputter CS 500 a 2·0-nm Pt layer was applied as well, but at room temperature. The particles in this layer appear slightly larger than those produced at − 120 °C. The agglomeration of particles is more intense, more pillar formation occurred, as can be seen in the FE-SEM image (Fig. 6a), and in the TEM image (Fig. 6b). The pillar formation is observable from the high contrast of many of the particles in the TEM image. As result of that there is more space between the individual agglomerates, suggesting a less continuous coating.

c With the VG Microtech SC 7640 Polaron sputter coater a

Fig. 5. Planar magnetron sputtered (Fisons-LT 7400 Cryo-unit) 2·0-nm Pt coating on carbon produced at − 120 °C; FE-SEM, 15 kV (a) and TEM, 100 kV (b). Note rather small reasonably uniformly shaped aggregates of particles Pt nuclei. Scale bar (see Fig. 10) = 50 nm.

Fig. 6. Planar magnetron sputtered (Fisons-500) 2·0-nm Pt coating on carbon produced at RT; FE-SEM, 15 kV (a) and TEM, 100 kV (b). Agglomerates are larger in size; packing density in TEM obviously lower. Scale bar (see Fig. 10) = 50 nm.

Fig. 7. Planar magnetron sputtered (VG Microtec SC 7640 Polaron) 2·0-nm Pt layer on carbon, produced at RT at 1·2 kV. In FE-SEM (a) rather large structures of Pt are observable; in TEM the particles or agglomerates appear rather small, uniform in size and closely packed. Scale bar (see Fig. 10) = 50 nm.

Fig. 8. Planar magnetron sputtered (VG Microtec SC 7640 Polaron) 1·0-nm Pt layer on carbon, similar to Fig. 7, but produced at RT at 800 V. Note the almost structureless image in FE-SEM at 15 kV and rather small and quite uniform Pt nuclei in the TEM at 100 kV. Scale bar (see Fig. 10) = 50 nm.

Fig. 9. Planar magnetron sputtered (Denton Oxford CT 1500 HF Cryo-transfer system) 2·0-nm Pt layer produced at RT. In FE-SEM at 15 kV almost no fine structure is observable; in TEM a close packing of small Pt nuclei, with some variation in height, is observable (compare with Fig. 8). Scale bar (see Fig. 10) = 50 nm.

Fig. 10. Planar magnetron sputtered (Cressington 208 HR) 1·5-nm Pt layer produced at RT. In FE-SEM at 15 kV almost no fine structure is observable; in TEM a close packing of small Pt nuclei, with some variation in height, is observable (compare with Fig. 8). Scale bar = 50 nm.

2·0-nm Pt layer was appied on carbon film at 1·2 kV. In the FE-SEM image (Fig. 7a), more or less globular structures are observable at an almost uniform grey background. In the TEM image (Fig. 7b) the particles do not appear as large but as average in size, more or less round to elongated and closely packed, with a slight difference in height. There is not much free space between the (agglomerates of) particles.
d With the VG Microtech SC 7640 Polaron sputter coater also a 1·0-nm Pt layer was applied on carbon film at 800 V, demonstrated in the FE-SEM image of Fig. 8(a). In comparison to the 2·0-nm layer almost no substructure can be seen in the FE-SEM image. The TEM image (Fig. 8b) of this 1·0-nm Pt layer shows a reasonably uniform division of particles. A closer view, using a magnifying glass, shows that the particle uniformity is less; the packing is, in view of the particle size, not as close as thought at first view. The particle size is smaller than in the case of the 2·0-nm layer, and the contrast is slightly lower, which could also indicate that few particles have grown in the direction perpendicular to the substrate. The background is more grey than in Fig. 7(b), indicating that may be very small amounts of material deposited between the particles, an effect seen before. What contributes most to the smaller coating particles, the thinner coating or the lower voltage applied, is not as yet clear.
e With the Denton planar magnetron cold sputter coating device, as subunit of the Oxford Instruments CT1500 HF Cryo-Transfer system, a 2·0-nm Pt layer on carbon film was produced at room temperature. In the FE-SEM image (Fig. 9a) almost no substructure can be distinguished. The surface structure in FE-SEM is not really different from the 1·0-nm layer observed in Fig. 8(a), while the layer is twice as thick. In the TEM image (Fig. 9b), there is a rather close packing of spherical as well as somewhat elongated particles. The highest contrast is seen with the more or less round particles; they seem to fill the available space quite well. The packing is closer than that of the 1·0-nm Pt layer of Fig. 8(b); at first view the particles appear slightly larger than in Fig. 9(b).
f With the Cressington 208 HR planar magnetron sputtering device a 1·5-nm Pt layer was produced at room temperature and short deposition distance on carbon film. The FE-SEM image of Fig. 10(a) shows almost no substructure at all. The TEM image (Fig. 10b) shows very small particles, even smaller than those seen in Fig. 8. Most appear as single, with a shape which can be described as slightly angular with rounded edges. The division is reasonably homogeneous; the background is rather grey, indicating more material in the background with a size not distinguishable with our TEM.

4. Magnetron sputtered Cr coatings on carbon film

a With the Cressington 208 HR planar magnetron sputtering device a 1·5-nm Cr layer was applied on carbon film at long deposition distance. In the FE-SEM image (Fig. 11a) almost no substructure is observable; the layer is not really different in appearance from the Au/Pd layer shown in Fig. 3. However, one should bear in mind that that layer has a thickness of only 1·5 nm. The chromium particles observed in the TEM image **(Fig. 11b)** are reasonably uniform in size and shape and tightly packed compared with the Au/Pd particles in Fig. 3(b), which appear somewhat elongated. The contrast of the Cr layer is rather low, owing to the low atomic number of Cr. In the TEM image a certain subdivision of groups of particles is observable.
b With the Edwards XE200 Xenosput chromium sputtering device a 1·5-nm Cr layer was deposited on a carbon substrate as well. In the FE-SEM image (Fig. 12a) the layer appears flat and homogeneous, with almost no substructure. In the TEM image (Fig. 12b) an extremely flat layer with no substructure can be seen. When the TEM image is observed more closely a similar subdivision is observable, but with a finer structure. Probably this subdivision of coating particles seen in FE-SEM and TEM images is a due to the sub structure of the carbon substrate.

5. Coatings on latex and cryo-surfaces

a With the Balzers BAE 120 high-vacuum evaporation unit a 2·0-nm Pt/C shadow coating was applied onto latex spheres which were deposited onto a carbon film (Fig. 13). The Pt nuclei are quite small, as is observable in the TEM image (b); they are even smaller than those seen in Figs. 5–10 at a comparable thickness. It seems that the combination Pt/C has a reducing effect on the size of the initial nuclei of Pt comparing Figs. 10(b) and 13(b).
b With an Edwards XE200 Xenosput planar magnetron sputtering device a 1·5-nm Cr coating was applied on latex particles (Fig. 14), showing a rather smooth and continuous layer. The FE-SEM image was taken at 15 kV accelerating voltage.
c In comparison with the Cr-coating of Fig. 13, a 1·5-nm Au/Pd-coating was applied onto a cryo-fractured face of a yeast cell (Fig. 15). Bakers' yeast was suspended in water overnight. A small clump of yeast was taken, excess of water removed with filter paper and slam frozen in liquid N_2 slush. The frozen sample was transferred to the Cryo Transfer System (Oxford CT 1500HF), fractured and coated by means of the Denton planar magnetron sputtering device. The membrane infoldings and the membrane particles are easily observable in this FE-SEM image, taken at 3 kV.

In Table 1 the results of the experiments have been summarized with reference to the figures. It shows that there is quite a difference in substructure of the various layers, even with the same coating material. These differences can be attributed to differences in the construction and working conditions of the instruments. The Cr

Table 1. Covering percentage and average particle surface area of various coatings and appearance of deposited layer.

Figure	Coating	Thickness (nm)	Density (%)*	Average area (nm^2)†	SD‡	Appearance	
1	Au/Pd	3·0	51	37			
2	Au/Pd	1·5	29	3		S§	T¶
3	Au/Pd	1·5	52	37	x	S	
4	Au/Pd	1·5	25	3		S	T
5	Pt	2·0	51	150	x		
6	Pt	2·0	49	200	x		
7	Pt	2·0	35	15	x		
8	Pt	1·0	30	7		S	T
9	Pt	2·0	42	22	x	S	
10	Pt	1·5	25	4		S	T
11	Cr	1·5	90	<0.5		S	T
12	Cr	1·5	100	<0.5		S	T
13	Pt/C	2·0	23	2		S	T

* Total area covered by particles divided by total area measured. †Average area of the particles (nuclei). ‡Layer with particle size with high standard deviation. §Smooth appearance in FE-SEM image. ¶Relatively smooth appearance in TEM image.

layers certainly show the smallest particle size, in fact so small that morphometric measurements could not detect them. A large difference in particle size is found between the particles of the various metal layers; the measurement of the average standard deviation clearly shows this difference. The average area of the particles does not show the differences in shape, only the differences in size; relatively large average areas indicate agglomeration of nuclei. Small average areas of the particles often give a low density (Table 1), but only the densest part of the particle is measured and often there is a gradient in thickness towards the sides which does not contribute to the morphometric calculations (Apkarian, 1994). Figure 11 shows cracks, probably due to the electron beam influence.

Discussion

The test with the conductive layers of Au/Pd, Pt and Cr, produced with different magnetron sputtering devices, was undertaken to investigate whether an Au/Pd coating could be used as an alternative to Au, Pt and particularly Cr in FE-SEM of tissues up to a magnification of approximately 200 000×. Au/Pd has the advantage of producing a large number of secondary electrons, owing to the different valencies of the Au atom. To exclude influences of specimen constituents and/or topography, a thin carbon film, evaporated onto freshly cleaved mica, was used as standard substrate in all tests. For microscopical observation, the carbon film was collected on 3·0-mm TEM copper grids and then sputter coated with the various metals. They were produced under the conditions set by the manufactures. Possibly fine tuning of certain parameters with respect to source–target distance, voltage and current could have changed the result slightly.

The use of low accelerating voltages in FE-SEM reduces charging and the need for an external conductive layer in comparison to high accelerating voltages; however, a conductive layer is still necessary to produce sufficient secondary electrons in the surface layer of the specimen and to protect the structure against radiation damage.

From the viewpoint of coating it is important to realize what type of specimen is investigated and at what resolution the coated specimens have to be examined. In the observation carried out in an FE-SEM with continuously variable working distance, a resolution of approximately 1·5–2·0 nm at 5–10 kV accelerating voltage is attainable at a short working distance of 4–6 mm. A so-called in-lens FE-SEM can operate at a resolution of better than 1 nm at 2–5 kV, while in a high-resolution STEM unit at high accelerating voltage resolutions of 0·7–1·0 nm can be obtained at very small spot sizes; Müller & Hermann, 1991; Wergin & Erbe, 1991; Pawley, 1992; Walther *et al.*, 1992).

Comparison of Au/Pd layers

The Au/Pd layers, produced with either an ion-beam sputtering device or a magnetron sputtering unit, vary slightly in thickness (1·5–3·0 nm). The dimensions of the Au/Pd particles in the ion-beam sputtered layer are larger than those produced with the magnetron sputtering devices, which is readily observable in the FE-SEM images. In FE-SEM the various Au/Pd coatings produced with magnetron sputter devices appear quite uniform, with no

subdivision in particles. The TEM images of these coatings had a different appearance. Figure 3(b) shows string-like agglomerated grains, tightly packed with only small open spaces between. The individual units forming the string seem to consist of very small grains. The coatings in Figs. 2(b) and 4(b) show Au/Pd particles embedded in a layer with much smaller particles (probably the initial Au/Pd grains), producing a more or less 'flat' grey contrast compared with that of Fig. 3(b). In both images a certain pattern is observable, a pattern already observed in the FE-SEM images. This 'cell-like' pattern is probably due to the special properties of the substrate.

In comparing the three Au/Pd coatings with approximately the same thickness, produced with a magnetron sputtering device, the Cressington and the Edwards devices produce the smallest particles; the space between those particles is filled with still smaller particles. The particles produced with the Denton device are larger, but closely packed; the particles seem to consist of agglomerations of more or less round particles. The FE-SEM image of the magnetron sputtered coatings does not show much difference in overall appearance.

Comparison of Pt layers

The Pt layers observed in FE-SEM, Figs. 8–10, with a varying thickness of 1·0–2·0 nm, appear similar. They show some kind of gross substructure, which was also observable in the FE-SEM images of Figs. 2–4. This is probably caused by the carbon substrate. When the coating particles are larger this effect is not visible. In TEM the Pt layers observed in Figs. 8–10 certainly differ in substructure, as observed in Figs. 2–4 for Au/Pd.

As indicated by the images in Figs. 5–10, there is also a large difference in appearance of the magnetron sputtered Pt layers, which is very obvious for Figs. 5 and 6 compared with Figs. 7–10. Obviously the Pt particles observable in Figs. 5 and 6 are larger in size than those in the other Pt coatings. There is a difference in particle size between the layers produced at cryo and room temperature, respectively, for the given sputtering apparatus (Echlin, 1992). The layer produced at cryo temperature contains smaller particles, which are more closely packed, so there is less open space between the agglomerates. At a closer view it seems that the individual particles with a somewhat angular shape agglomerate, forming a kind of string; in the FE-SEM images this difference was already observable.

The FE-SEM image obtained at room temperature (Fig. 6a) resembles the Au coatings from the past, produced with diode sputtering devices at relatively low vacuum.

The Pt coating observable in Fig. 7 shows a structure of its own, in contrast to those of Figs. 8–10. The shape of the particles is difficult to observe in the FE-SEM image; the TEM image, however, shows a closely packed arrangement of somewhat angular, sometimes slightly elongated, but mostly separate particles. The layer thickness is 2·0 nm compared with the 1·0-nm layer of Fig. 8 produced with the same instrument under slightly different conditions. The difference in layer appearance between Fig. 7 and Fig. 8 is due to the voltage employed at sputtering. Figure 8 is produced at 800 V, while Fig. 7 is produced at 1·2 kV, both with the same instrumentation. Figure 8(b) clearly shows the initial Pt coating particles, somewhat angular in shape and reasonably equal in size. In the background much smaller particles can just be discerned, taking account of the somewhat grey but uniform background. When the layer thickness increases from 1·0 to 2·0 nm the individual particles grow both at the sides and in height, at the expense of the very small particles forming the background. In the 2·0-nm layer the spaces between the particles appear much clearer; there are no longer any particles in the background.

Comparison of Au/Pd, Pt and Cr layers

One of our findings is that the quality of the Au/Pd, Pt and Cr layers, as judged from the parameters discussed above, varies with the type of magnetron sputtering device used. That the temperature at which the layer is applied (the temperature of the substrate) affects the particle size and chances for agglomeration was known already. Layers produced at low temperature have a slightly smaller particle size and a lower tendency to agglomeration than those produced at room temperature, which is in agreement with earlier findings (Echlin, 1992).

Chromium is a must in (ultra) high-resolution work of

Fig. 11. Planar magnetron sputtered (Cressington 208) 1·5-nm Cr-coating on carbon; FE-SEM, 15 kV (a) and TEM, 100 kV (b). Note very small Cr nuclei forming a continuous flat layer. Scale bar (see Fig. 12) = 50 nm.

Fig. 12. Planar magnetron sputtered (Edwards XE200 Xenosput) 1·5-nm Cr coating on carbon; FE-SEM, 15 kV (a) and TEM, 100 kV (b). Very smooth continuous flat layer. Scale bar = 50 nm.

Fig. 13. High-vacuum evaporated (Balzers BAE 120) 2·0-nm Pt coating on latex particles on carbon; so-called shadow coating; FE-SEM 15 kV (a) TEM 100 kV (b). Scale bars = 100 nm (a), 50 nm (b).

Fig. 14. Planar magnetron sputtered (Edwards XE200 Xenosput) 1·5-nm Cr coating on latex particles on carbon; FE-SEM at 15 kV. Note quite smooth surface with no obvious substructures observable. Scale bar = 100 nm.

Fig. 15. Planar magnetron sputtered (Denton Oxford CT 1500HF Cryo transfer system) 1·5-nm Au/Pd coating, produced at − 120 °C, on a yeast cell fracture face showing membrane particles. Scale bar = 100 nm.

membranes, for example thin layers; moreover, it is necessary in X-ray microanalysis because it does not interfere much with the K lines of most constituents of biological materials such as phosphorus and calcium. No X-ray microanalyses were carried out by us on the chromium coatings to check for the presence of chromium oxides. Chromium produces a very smooth coating with no substructure observable, although with relatively low contrast (Apkarian, 1994). However, there are a few drawbacks to the use of chromium as a coating material for biological specimens in FE-SEM, such as the purity of the chromium target, the high vacuum required, the purity of

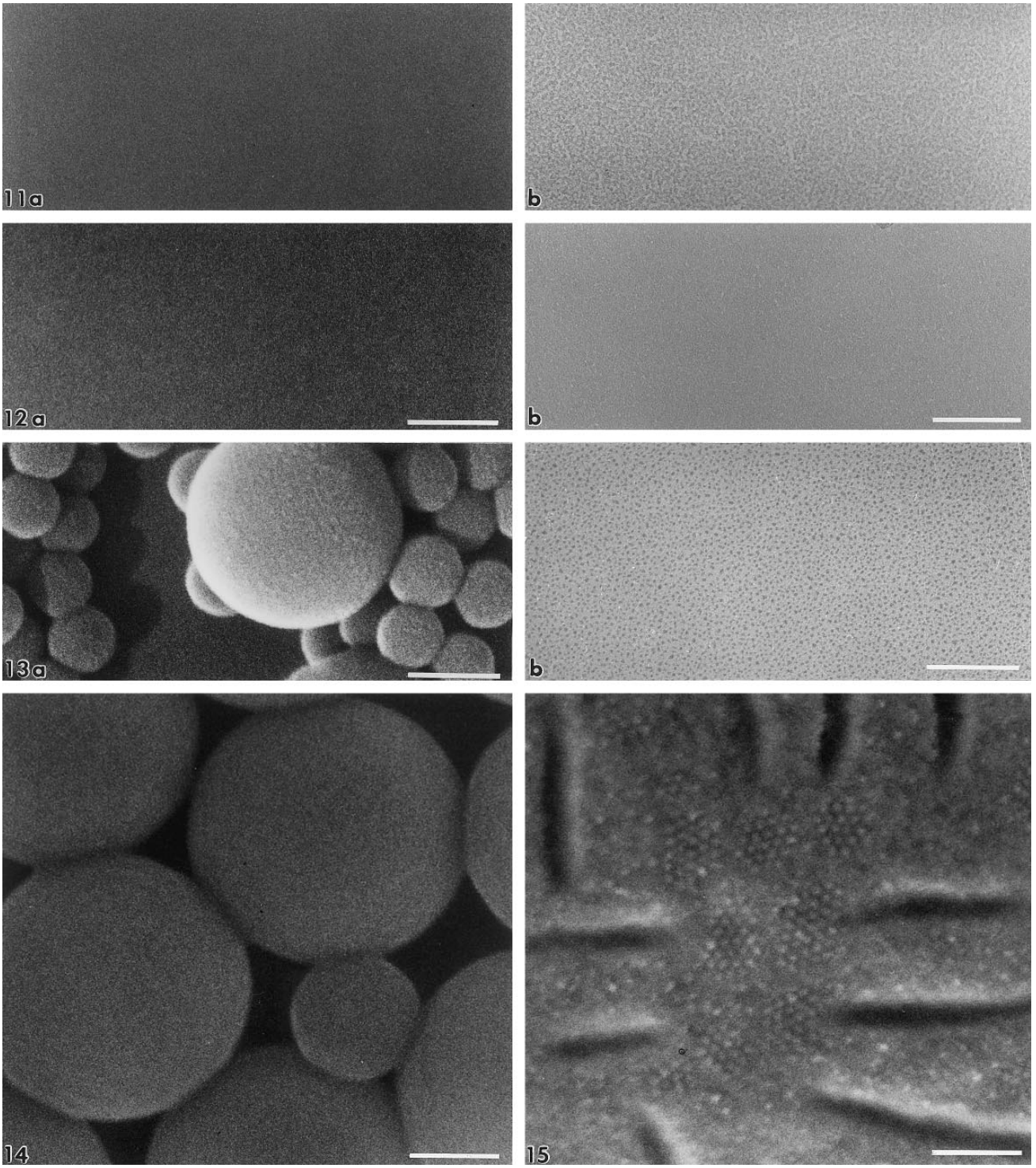

the inert gas used, the lower secondary electron emission of chromium compared with Au/Pd and Pt, and the rapid oxidation of the coating layer surface. Chromium can oxidize rapidly, so it should be stored permanently in a vacuum; needless to say, a clean vacuum is a first priority, together with pure argon gas to prevent contamination of both the chromium target and the coating. A special bottle with high-purity argon gas screwed onto the system ensuring a metal–metal contact will function the best (Echlin, 1992).

Apart from the substructure of the coating due to agglomeration of coating particles, as clearly seen in the FE-SEM images shown in Figs 1, 5, 6 and 7, a weak pattern is observable, particularly in Figs. 2–4 and 8–12, which could be attributed to the the carbon background because in all cases this pattern is similar.

Differences in instrumentation and operation temperature

The question becomes relevant whether special conditions for a particular instrument favour the formation of very small grains or just the opposite (Hermann *et al.*, 1988). It is obvious that the relatively low vacuum conditions in the diode-sputtering promote the existence of larger grains of Au which grow to larger agglomerates with increasing thickness of the layer and/or as a result of electron beam irradiation in the microscope. Breaking the vacuum after deposition also increases possibilities of agglomeration.

Ultrathin coatings for use at ultra high-vacuum (UHV) conditions have been discussed by Gross *et al.* (1984). Obviously, collisions between the coating particles and the inert gas (argon, xenon) molecules are limited with respect to low-vacuum sputtering, so rotation of the specimen has to be carried out to avoid shadow effects. In this respect magnetron sputtering devices certainly are better than ion-beam sputtering devices with or without rotation of the sample. For (S)TEM investigations thin Pt, Ta/W or W films are often used in combination with rotary shadowing at high elevation angles (approximately 65°) (Ruben, 1989; Wepf & Gross, 1990; Wepf *et al.*, 1991). Grain structures in these films with a height of approximately 1–1·5 nm and a lateral width of approximately 1·5–3·0 nm could be measured in high-resolution STEM; these data are certainly important at (ultra) high-resolution work, STEM and in-lens FE-SEM (Apkarian *et al.*, 1990; Joy, 1990; Herman & Muller, 1991a,b).

Observation of the coating nuclei in freeze fracture faces of biological samples such as yeast cells is more difficult than for simple carbon film substrates. One of the reasons is the possibility of contamination by water vapour, which can cause a decoration effect, a problem already observed in freeze fracture/replicas in TEM by Gross *et al.* (1978). The plasmic fracture face of yeast plasmalemma (PF-face) in Fig. 15 shows clearly the membrane particles after Au/Pd coating at cryo temperature; there are no artefacts due to preparation or beam irradiation observable.

An appropriate comparison between cryo- and ambient temperature is also shown in Figs. 5 and 6, carried out with the same sputtering device for the same coating material and in a layer of the same thickness, an effect studied by Müller *et al.* (1990) and Wergin *et al.* (1993). Another effect could be the breaking of the vacuum; in cryo-experiments the vacuum is not broken after sputtering.

Conclusions

1 As already found by others, there are differences in size, shape, height and density of the particles in layers of the same thickness of the various metals tested. Obviously cryo-temperatures slow down the growth of nuclei and the agglomeration process of the grains.

2 Even for coatings of the same metal with the same thickness, obtained by means of different magnetron sputtering devices, there are differences in particle size, shape and density. The particular construction of the sputtering devices, with source–target distance, cleanness of the vacuum and argon gas, voltage employed and substrate temperature, play an important role in the final result.

3 For biological structures to be studied with an FE-SEM with a continuously variable working distance, an Au/Pd coating, produced with the appropriate magnetron sputtering device, can be a good alternative for Pt and Cr coatings.

Acknowledgments

We wish to thank Mr T. King and Ir C. J. M. Braun, Fisons Instruments; VG Microtech, Uckfield, East Sussex, U.K. and MSI, Bergen op Zoom, The Netherlands; Mr A. Robins, Oxford Instruments, Oxford, U.K.; Mr J. P. Vermeulen from Elektronen Optik Service, Dortmund, Germany, and Mr T. Schouten and Mr J. Donders, de Jong Groep, Rotterdam (Edwards) for the use of their sputter coating units and cryo systems, advice, valuable help and hospitality.

References

Apkarian, R.P. (1994) Analyses of high quality monatomic chromium films used in biological high resolution scanning electron microscopy. *Scanning Microsc.* **8**, 289–301.

Apkarian, R.P., Gutekunst, M.D. & Joy, D.C. (1990) High resolution SE-I SEM study of enamel crystal morphology. *J. Electron Microsc. Technique*, **14**, 70–78.

Echlin, P. (1992) *Low Temperature Microscopy and Analysis*. Plenum Press, New York.

GATAN. (1997) *Know-How Newsletter for Electronmicroscopy. New Precision Etching and Coating, Vol. 4 (2), 1*. Gatan Ltd, 17 Medicott Close, Oakley Hay, Corby NN18 9NF, UK.

Gross, H., Krusche, K. & Tittman, P. (1990) Recent progress in high

resolution shadowing for biological transmission electron microscopy. In: *Proc. XIIth Int. Congr. for EM, Seattle*. San Francisco Press, San Francisco.

Gross, H., Kubler, O., Bas, E. & Moor, H. (1978) Decoration of specific sites on freeze-fractured membranes. *J. Cell Biol*. **79,** 646–656.

Gross, H., Muller, T., Wildhaber, I. & Winkler, H. (1985) High resolution metal replication quantified by image processing of periodic test specimens. *Ultramicroscopy*, **16,** 287–304.

Gross, H., Müller, T., Wildhaber, I., Winkler, H. & Moor, H. (1984) Freeze fracturing and replication at −260 C. *Proc. 42nd Annual Meeting of Electron Microscopy Society of America*. San Francisco Press, San Francisco.

Hermann, R. & Müller, M. (1991a) High resolution biological scanning electron microscopy. *J. Electron Microsc. Technique*, **18,** 440–449.

Hermann, R. & Müller, M. (1991b) Prerequisites of high resolution scanning electron microscopy. *Scanning Microsc*, **5,** 653–664.

Hermann, R., Pawley, J., Nagatini, T. & Müller, M. (1988) Double axis rotary shadowing for high resolution scanning electron microscopy. *Scanning Microsc*. **2,** 1215–1230.

Jongebloed, W.L., Dunnebier, E., Albers, F.J.W. & Kalicharan, D. (1996) Visualization of the fine structure of stereocilia of the organ of corti of the guinea pig by FEG-SEM; variations in fixation technique and accelerating voltage. *Scanning Microsc*. **10,** 147–164.

Jongebloed, W.L., Kalicharan, D. & Worst J.G.F. (1994) High resolution FEG-SEM images of biological tissue.*Proc 13th Int. Conf. EM Paris*, Vol. 3a, pp. 777–778.

Joy, D.C. (1990) Contrast in high resolution scanning electron microscope images. *J. Microsc*. **161,** 343–355.

Kalicharan, D., Jongebloed, W.L., Los, L.I. & Worst, J.G.F. (1992) Application of tannic acid non-coating technique in eye research: lens capsule and cataractous lens fibres. *Beitr. Elektronenmikroskop. Direktabb. Oberfl*. **25,** 201–205.

Müller, T., Gross, H., Winkler, H. & Moor, H. (1985) High resolution shadowing with pure carbon. *Ultramicroscopy*, **16,** 340–348.

Müller, M. & Hermann, R. (1991) Towards high resolution SEM of biological objects. *Hitachi Instr. News*, **19,** 50–57.

Müller, T., Walther, P., Scheidegger, C., Reichelt, R., Müller, S. & Guggenheim, R. (1990) Cryo-preparation and planar magnetron sputtering for low temperature scanning electron microscopy. *Scanning Microsc*. **4,** 863–876.

Oxford Instruments, Scientific Research Division Research Instruments. (1995) *Oxford EM Applications Note*: High resolution freeze fracture in the SEM.

Pawley, J.B. (1992) LVSEM for high resolution topographic and density contrast imaging. *Adv. Electron Electron Phys*. **83,** 203–275.

Peters, K.R. (1984) Continuous ultrathin metal films. *The Science of Biological Specimen Preparation for Microscopy and Microanalysis* (ed. by J. P Revel, T. Barnard and G. H. Haggis), pp. 221–231. Scanning Electron Microscopy Inc., AMF O'Hare, Chicago.

Peters, K.R. (1986) Metal coating and image quality in scanning electron microscopy. *Proc. 44th Ann. Meet. Electron Microsc Soc Am.* pp. 70–71. San Francisco Press, San Francisco.

Ruben, G.C. (1989) Ultrathin (1 nm) vertically shadowed platinum-carbon replicas for imaging individual molecules in freeze-etched biological DNA and material science metal and plastic specimens. *J. Electron Microsc. Technique*, **13,** 335–354.

Walther, P., Chen, Y., Peach, L.L. & Pawley, J.B. (1992) High resolution scanning electron microscopy of frozen-hydrated cells. *J. Microsc*. **168,** 169–180.

Wepf, R., Amrein, M., Burkli, U. & Gross, H. (1991) Platinum/iridium/carbon: a high resolution shadowing material for TEM, STM and SEM of biological macromolecular structures. *J Microsc*. **163,** 51–64.

Wepf, R. & Gross, H. (1990) Part /Ir/C a new powerfull coating material for high resolution SEM. *Proc. XIIth Int Congr. for EM Seattle*, San Francisco Press, San Francisco.

Wergin, W.P. & Erbe, E.F. (1991) Increasing resolution and versatility in low temperature conventional and field emission scanning electron microscopy. *Scanning Microsc*. **5,** 927–936.

Wergin, W.P., Erbe, E.F. & Robins, A. (1993) Use of platinum shadowing and magnetron coating in an Oxford Cryotransfer system to increase low temperature resolution of biological samples in a Hitachi field-emission scanning electron microscope. *Proc. 51st Ann. Meet. Microsc. Soc. Am.* p. 122. San Francisco Press, San Francisco.